

# Measurement of the Spin-forbidden Decay rate $(3s3d)^1D_2 \rightarrow (3s3p)^3P_{2,1}$ in $^{24}\text{Mg}$

K. T. Therkildsen,\* B. B. Jensen, C. P. Ryder, N. Malossi, and J. W. Thomsen

*The Niels Bohr Institute, Universitetsparken 5, 2100 Copenhagen, Denmark*

(Dated: November 2, 2018)

## Abstract

We have measured the spin-forbidden decay rate from  $(3s3d)^1D_2 \rightarrow (3s3p)^3P_{2,1}$  in  $^{24}\text{Mg}$  atoms trapped in a magneto-optical trap. The total decay rate, summing up both exit channels  $(3s3p)^3P_1$  and  $(3s3p)^3P_2$ , yields  $(196 \pm 10) \text{ s}^{-1}$  in excellent agreement with recent relativistic many-body calculations of [S.G. Porsev et al., Phys. Rev. A. **64**, 012508 (2001)]. The characterization of this decay channel is important as it may limit the performance of quantum optics experiments carried out with this ladder system as well as two-photon cooling experiments currently explored in several groups.

PACS numbers: Valid PACS appear here

---

\*Electronic address: kaspertt@fys.ku.dk

## I. INTRODUCTION

The interest in alkaline earth systems has increased significantly over the past years. One of the main interests in these systems is their applications to high resolution spectroscopy and atomic frequency standards, as they offer very narrow electronic transitions [1]. Another attractive feature of the two-electron systems is their very simple energy level structure, for bosonic isotopes, free of both fine and hyperfine structure. This simple structure opens for detailed comparison between theory and experiment [2]. Recent advances in *ab initio* relativistic many-body calculations of two-electron systems have provided very accurate values for atomic structure and properties such as the electric-dipole transitions of Mg, Ca, and Sr[3]. However, in the case of Mg relatively few experiments have been reported in literature motivating the studies in this Brief Report.

In a series of papers two photon cooling in ladder schemes have been proposed to lower the temperature below the doppler limit of alkaline earth elements [4, 5, 6]. The magnesium and calcium systems are of particular interest since cooling is limited to a few mK. Experimental evidence for two-photon cooling has been established, but the effect is rather modest contrary to theoretical predictions [7, 8]. One important mechanism to take into account in these studies are leaks from the ladder system, limiting the number of atoms that eventually can be cooled.

In this this Brief Report we present the first measurements of the spin forbidden decay from the magnesium  $(3s3d)^1D_2$  state to  $(3s3p)^3P_1$  and  $(3s3p)^3P_2$ . Using atoms trapped in a magneto-optical trap we optically prepare the atoms in the  $(3s3d)^1D_2$  state and measure the decay to  $(3s3p)^3P_{2,1}$  manifold by trap loss measurements. This enables us to deduce the absolute decay rate for these transitions and compare our results to state of the art theoretical calculations.

## II. TRAP LOSS MEASUREMENTS

In figure 1, we show the relevant energy levels and transitions in our experiment. The 285 nm transition is used for cooling and trapping the atoms while the 881 nm transition is used to populate the  $(3s3d)^1D_2$  state. From this state the atoms may decay to the  $(3s3p)^3P_1$

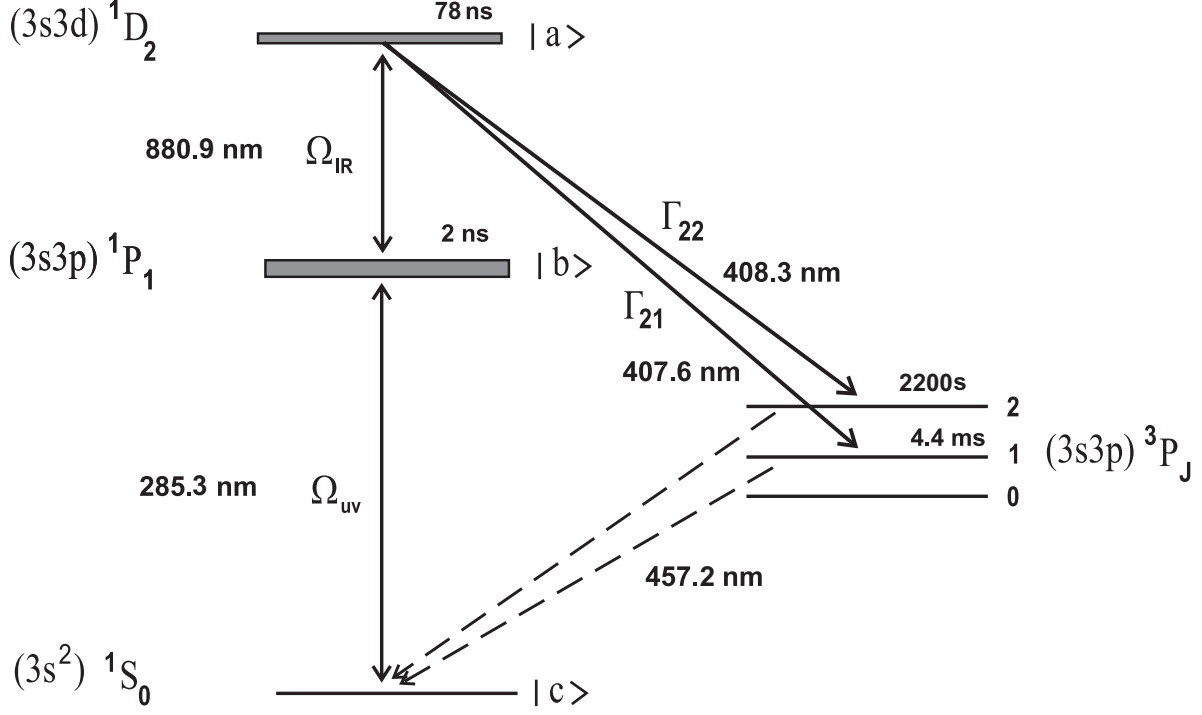


FIG. 1: Energy levels relevant for the  $(3s3d) \ ^1D_2 \rightarrow (3s3p) \ ^3P_{2,1}$  decay measurement in  $^{24}\text{Mg}$ .

state ( $407.6 \text{ nm}$ ) with rate  $\Gamma_{21}$  or to the  $(3s3p) \ ^3P_2$  state ( $408.3 \text{ nm}$ ) with rate  $\Gamma_{22}$ , or simply back to  $(3s3p) \ ^1P_1$ . By neglecting decay to the  $(3s3p) \ ^3P_0$  state, which is weaker by orders of magnitude, no other decay channels are open. When the  $881 \text{ nm}$  laser is switched off we express the steady state number of atoms  $N_0$  as the ratio of the load rate to linear losses  $L/\alpha$ . Here we neglect intra-MOT collisions since we are working at relative low atom densities. The equation for the number of atoms trapped in the MOT with  $881 \text{ nm}$  light present can be written as:

$$\dot{N} = L - \rho_{aa} (\Gamma_{22} + \Gamma_{21})N - \alpha N. \quad (1)$$

Experimentally we determine the total loss rate  $\Gamma_{22} + \Gamma_{21}$ . In our case the linear loss rate  $\alpha$  is dominated by resonant photo-ionization of  $(3s3p) \ ^1P_1$  at  $285 \text{ nm}$  [9]. Photo-ionization from the  $(3s3d) \ ^1D_2$  level is below  $1 \text{ Mb}$  and will not be considered here[10]. The steady state becomes

$$N^{on} = \frac{L}{\rho_{aa} (\Gamma_{22} + \Gamma_{21}) + \alpha^{on}}, \quad (2)$$

and

$$N^{off} = \frac{L}{\alpha^{off}}. \quad (3)$$

The ratio of signal with 881 nm turned on and off is proportional to  $\rho_{bb}^{on}$ ,  $\rho_{bb}^{off}$  respectively.

We find finally

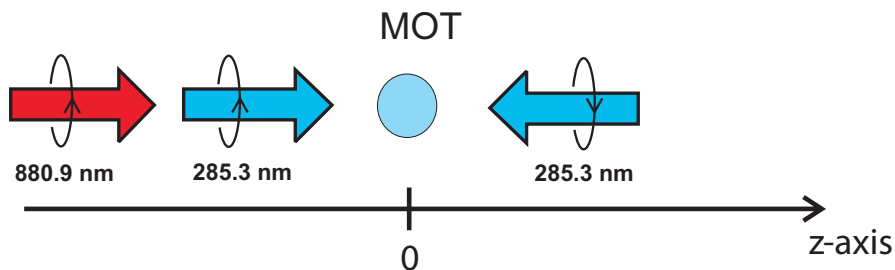
$$\frac{S^{on}}{S^{off}} = \frac{\alpha^{off} \rho_{bb}^{on} / \rho_{bb}^{off}}{\rho_{aa} \left( \Gamma_{21} + \Gamma_{22} \right) + \alpha^{off} \frac{\rho_{bb}^{on}}{\rho_{bb}^{off}}}, \quad (4)$$

as the  $\alpha$ -coefficient is dominated by resonant photo-ionization and thus proportional to the fraction of atoms in the  $(3s3p)^1P_1$  state. So far we assumed that all atoms decaying to the  $(3s3p)^3P_J$  manifold are lost. This is indeed the case for the  $(3s3p)^3P_2$  final states due to their long lifetime exceeding 2200 seconds [11]. On the time scale of the experiment, being only a few seconds, we consider the atoms from this state lost. However, for the  $(3s3p)^3P_1$  states atoms in the  $|J = 1, m_j = +1\rangle$  magnetic sub state will be trapped in the magnetic quadrupole field of the MOT and most likely be recaptured when decaying back to the  $(3s^2)^1S_0$  ground state. Atoms in  $|J = 1, m_j = 0, -1\rangle$  magnetic sub states are expected to be lost since the rms velocity of the trapped atoms exceed 1 m/s leading to a rms travelled distance of more than 5 mm, which is large compared to our MOT beam diameter of only a few mm. The total decay rate will thus be modified to  $\gamma\Gamma_{21} + \Gamma_{22}$ . The actual value of  $\gamma$  depend strongly on the polarization of the 285 nm beam and the 881 nm beam.

If we assume a standard one dimensional model for the MOT we can determine the influence of the constant  $\gamma$ . This is a good approximation as the 881 nm beam is directed along one of the uv MOT beams, but not retro reflected. Consider atoms on the  $-z$  side, see figure 2. These atoms will mainly populate the  $|J = 1, m_j = 0, -1\rangle$  state. Further excitation of the collinear 881 nm laser will drive the atoms to the left (blue line) or right (red line) depending on the helicity of the 881 nm laser. This creates an anisotropy in the decay to the  $(3s3p)^3P_1$  state. Atoms driven along the blue line, i.e., with same polarization helicity as the MOT beams, will only populate non-trapped states. Experiments performed in this configurations is thus insensitive to the re-trapping dynamics as described above. Using the Clebsch Gordan coefficients shown in figure 2 we find the rate  $(1/2 \cdot 1 + 1/2 \cdot (1/2 + 1/2))\Gamma_{21} = \Gamma_{21}$ , as expected. For the opposite polarization we find a reduction  $(1/2 \cdot 1/2 + 1/2 \cdot (2/3 + 1/6))\Gamma_{21} = 2/3\Gamma_{21}$ . We now Consider a more general case where all three magnetic sub states  $|J = 1, m_j = +1, 0, -1\rangle$  are populated. The populations are denoted  $n_+$   $n_0$  and with  $n_+ + n_0 + n_- = 1$ . We find the effective decay constant as  $(1 - n_+/6)\Gamma_{21}$  for MOT polarization. The  $n_+$  coefficient is expected to be small compared to the sum of the two other terms. However, even in an extreme case where all sub states

are populated equally  $\Gamma_{21}$  is effected only by about 5%.

(a)



(b)

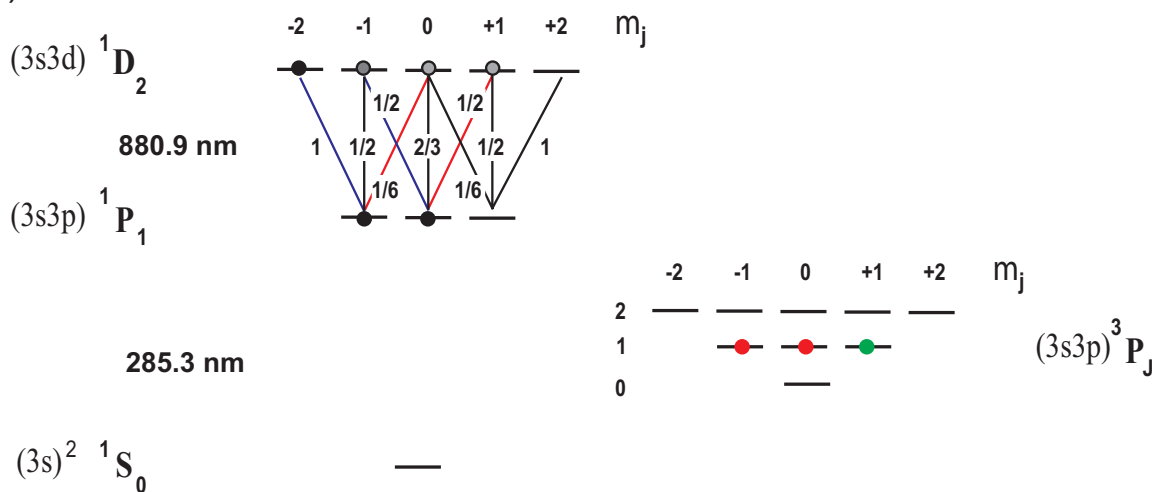


FIG. 2: (color online)(a) Experimentally the 881 nm beam is co-linear with one of the MOT beams. The polarization state can be selected similar to the MOT helicity, as shown in the figure, or opposite. (b) Polarization dependent pumping of atoms in the MOT. Assuming a one dimensional representation of the MOT the 881 nm polarization, represented by blue line (= MOT helicity) or red line, optical pumping will drive the atoms such that anisotropy in the decay rate will emerge. The green dot represents atoms trapped in the MOT quadrupole magnetic field, while red dots represents atoms in non-trapped states. The Clebsch Cordan coefficients shown will also apply to the  $(3s3d) \ ^1D_2 \rightarrow (3s3p) \ ^3P_1$  decay.

With a 881 nm helicity opposite to that of the MOT beam, marked in red color on figure 2, will ultimately result in a destruction of the trapping force as the 881 nm laser intensity increases. This effect is expected as a result of destructive reshuffling of the atoms into "wrong" magnetic sub states.

### III. EXPERIMENTAL SETUP AND RESULTS

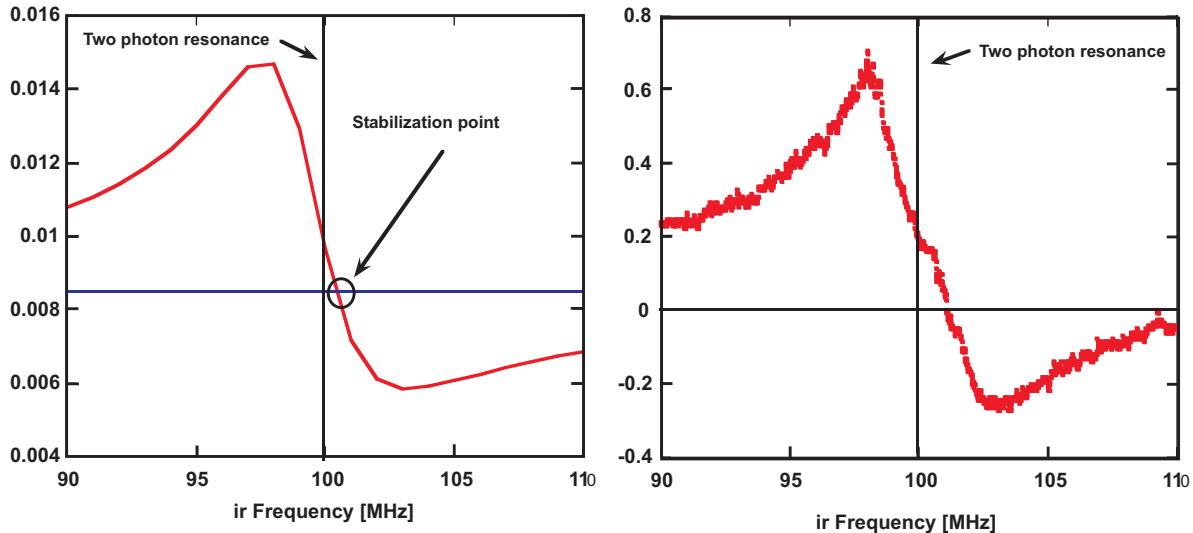


FIG. 3: (color online) The 881 nm laser is frequency locked to the two photon resonance of the ladder system  $\nu_{881} = -\nu_{285} = 100$  MHz. This ensures a maximal transfer of population to the  $(3s3d) \ ^1D_2$ . Left part of the figure shows the  $(3s3p) \ ^1P_1$  excited state fraction obtained from the optical Bloch equations. Right part shows the experimental lock signal.

The main part of the experimental setup has been described in [12]. In our experiment the 285 nm MOT is probed by 881 nm light produced by a Ti:Sapphire laser. The 881 nm light is power and frequency controlled by an AOM. A  $\lambda/4$  plate controls the helicity of the light. Presence of the 881 nm light will change the 285 nm light level recorded by a PM (not sensitive to 881 nm light). This we use to lock the 881 nm laser frequency close to the two photon resonance  $\nu_{881} = -\nu_{285} = 100$  MHz during the experiments, see figure 3. Increasing the rabi frequency of the 881 nm light causes a minor change in the locking point. In our power range this corresponds to about 1 MHz and not considered important at this level of accuracy.

Typically  $10^7$  atoms are captured in the MOT, with a rms diameter of 1 mm and temperatures from 3 to 5 mK. The Doppler cooling limit for the MOT is 2 mK as sub-Doppler cooling is not supported in this system.

The number of emitted 285 nm photons when the ir laser was on and off respectively, was measured for each of the two circular polarizations states. The 881 nm light was sent through the AOM, which was modulated with a square wave at 1 kHz, with a duty cycle

of 20 %. The photomultiplier signal was measured and average over 32 periods with the light respectively on and off, thus providing values for  $S^{on}$  and  $S^{off}$ . At the same time these signals provided a lock of the Ti:S laser to the two photon resonance, see figure 3. This measurement was repeated for different ir intensities (Rabi frequencies), while the MOT was running in steady state mode.

Experimental values for the ratio  $\frac{S^{on}}{S^{off}}$  as a function of the 881 nm Rabi frequency are show in figure 4. As expected the fraction starts out at 1 and gradually decreases as the Rabi frequency is increased. In figure 4 the 881 nm polarization corresponds to the MOT helicity (blue line in figure 2) and polarization opposite to the MOT helicity. The solid curves are results from a simulation based on the optical Bloch equations including the MOT magnetic field. Experiments with this helicity clearly supports a value of  $\Gamma = (196 \pm 10) \text{ s}^{-1}$  in good agreement with calculations performed in [3], where  $\Gamma = \Gamma_{22} + \Gamma_{21} = (57.3 + 144) \text{ s}^{-1}$ . For the opposite 881 nm polarization (red line in figure 2) we observe a reduced decay constant of  $\Gamma = (150 \pm 15) \text{ s}^{-1}$ . Using values of [3] and the coefficient deduced above we obtain  $\Gamma = \Gamma_{22} + 2/3\Gamma_{21} = 153 \text{ s}^{-1}$  in favor of the one dimensional model described above. From this we find the decay constants  $3s3d^1D_2 \rightarrow 3s3p^3P_1$ , and  $3s3d^1D_2 \rightarrow 3s3p^3P_2$  to be  $\Gamma_{21} = 138 \pm 10 \text{ s}^{-1}$  and  $\Gamma_{22} = 58 \pm 4 \text{ s}^{-1}$ .

#### IV. CONCLUSION

In conclusion we have measured the total spin forbidden decay rate  $(3s3d)^1D_2 \rightarrow (3s3p)^3P_{2,1}$  in  $^{24}\text{Mg}$ . We find a rate of  $\Gamma = (196 \pm 10) \text{ s}^{-1}$  supporting state of the art relativistic many-body calculations. Assuming a simple one dimensional model for the MOT we find the differential decay constants  $(3s3d)^1D_2 \rightarrow (3s3p)^3P_1$ , and  $(3s3d)^1D_2 \rightarrow (3s3p)^3P_2$  as  $\Gamma_{21} = 138 \pm 10 \text{ s}^{-1}$  and  $\Gamma_{22} = 58 \pm 4 \text{ s}^{-1}$  supporting the above mentioned calculations.

With a total loss rate of  $196 \text{ s}^{-1}$  the magnesium MOT lifetime can be limited to milliseconds time scale or less near the two photon resonance. To avoid significant atom losses the cooling time of a two-photon cooling scheme must be kept below 1 ms, as demonstrated in [8]. The losses from the  $^1D_2$  state are according to [5],[6] limiting the minimum temperature reachable by two-photon cooling to about  $50 \mu\text{K}$ . In quantum optics experiments employing this ladder system decoherence will likewise play a role on relative short timescales.

However the decay rate  $\Gamma_{22}$  opens a way of populating the  $^3P_2$  state. For our current

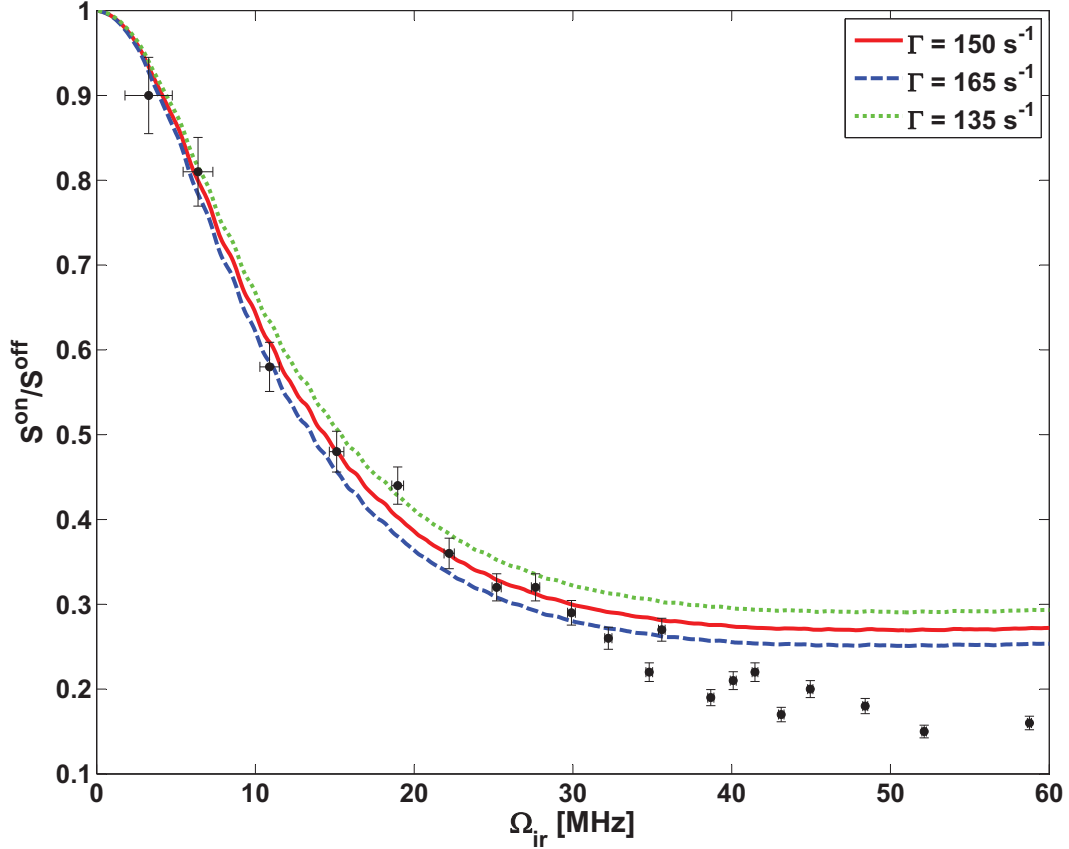
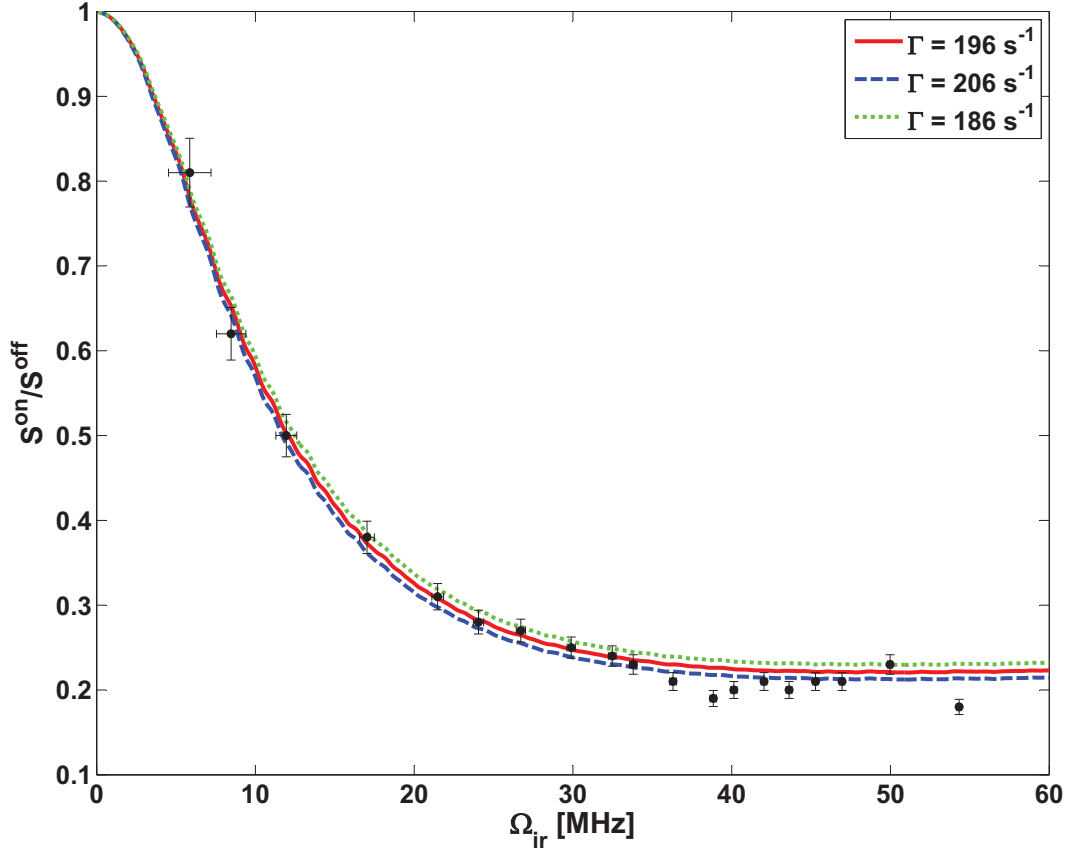


FIG. 4: (color online) Experimental values for the ratio  $\frac{S^{\text{on}}}{S^{\text{off}}}$  as a function of the 881 nm Rabi frequency. (top) Here the circular polarization  $\hat{s}$  corresponds to the MOT helicity (blue lines in figure 2). The curves are results from a simulation based on the optical Bloch equations, including the



MOT characteristics a load rate in the order of  $10^5 - 10^6$  atoms/s is expected. Assuming a magnetic trap lifetime in the order of 20 s, this will result in a  $^3P_2$  population of  $10^6 - 10^7$  atoms. However, the loading rate into the  $^3P_2$  can be increased by increasing the MOT loading rate using a Zeeman slower. The  $^3P_2$  state is a fine starting point for further laser cooling on the  $^3P_2 - ^3D_3$  transition as done for Ca [13].

### Acknowledgments

We wish to acknowledge the financial support from the Lundbeck Foundation and the Carlsberg Foundation.

- 
- [1] T. P. Heavner, S. R. Jefferts, E. A. Donley, J. H. Shirley, T. E. Parker, *Metrologia* **42**, 411 (2005).  
S. Bize et al., *J. Phys. B* **38**, S449 (2005)  
L. Hollberg et al., *J. Phys. B* **38**, S469 (2005)  
M. M. Boyd et al., *Science* **314**, 1430 (2006)  
W. H. Oskay et al., *Phys. Rev. Lett.* **97**, 020801 (2006)
- [2] Mette Machholm, Paul S. Julienne and Kalle-Antti Suominen. *Phys. Rev. A.* **59**, R4113 (1999)
- [3] Porsev, S. G. and Kozlov, M. G. and Rakhlina, Y. G. and Derevianko, A. *Physical Review A* **64**, 012508 (2001)
- [4] Wictor C. Magno, Reinaldo L. Cavasso Filho, and Flavio C. Cruz. *Phys. Rev. A* **67**, 043407 (2003)
- [5] Josh W. Dunn, J. W. Thomsen, Chris H. Greene, and Flavio C. Cruz. *Phys. Rev. A* **76**, 011401(R) (2007)
- [6] Giovanna Morigi and Ennio Arimondo. *Phys. Rev. A* **75**, 051404(R) (2007)
- [7] N. Malossi, S. Damkjær, P. L. Hansen, L. B. Jacobsen, L. Kindt, S. Sauge, J. W. Thomsen, F. C. Cruz, M. Allegrini, and E. Arimondo. *Phys. Rev. A* **72**, 051403 (2005)
- [8] T. E. Mehlstäubler, K. Moldenhauer, M. Riedmann, N. Rehbein, J. Friebe, E. M. Rasel, and W. Ertmer. *Phys. Rev. A* **77**, 021402(R) (2008)
- [9] Madsen D. N. and Thomsen J. W. *J. Phys. B* **33**, 4981 (2000)

- [10] T. K. Fang, T. N. Chang Physical Review A **61**, 052716 (2000)
- [11] Sergey G. Porsev and Andrei Derevianko. Phys. Rev. A **69**, 042506 (2004)
- [12] Loo F. Y., Bruschi A., Sauge S., Allegrini M., Arimondo E., Andersen N., Thomsen J. W. J. Opt. B: Quantum Semiclass. Opt. **6**, 81 (2004)
- [13] C. Y. Yang, P. Halder, O. Appel, D. Hansen, and A. Hemmerich, Phys. Rev. A **76**, 033418 (2007)